



**SPARSE model for
the prediction of
evapotranspiration
from TIR data**

G. Boulet et al.

The SPARSE model for the prediction of water stress and evapotranspiration components from thermal infra-red data and its evaluation over irrigated and rainfed wheat

G. Boulet^{1,2}, B. Mougenot^{1,2}, J.-P. Lhomme³, P. Fanise¹, Z. Lili-Chabaane^{2,4}, A. Olioso^{5,6}, M. Bahir^{1,5,6}, V. Rivalland¹, L. Jarlan¹, O. Merlin¹, B. Coudert¹, S. Er-Raki⁷, and J.-P. Lagouarde⁸

¹CESBIO – UMR 5126 UPS, CNRS, CNES, IRD, Toulouse, France

²Département Génie Rural des Eaux et Forêts, Institut National Agronomique de Tunisie, Tunis, Tunisia

³IRD, UMR LISAH, Montpellier, France

⁴Université de Carthage, Tunis, Tunisia

⁵INRA, EMMAH – UMR1114, Avignon, France

⁶UAPV, EMMAH – UMR1114, Avignon, France

⁷LP2M2E, FST, Université Cadi Ayyad, Marrakech, Morocco

Title Page

Abstract

Introduction

Conclusions

References

Tables

Figures



Back

Close

Full Screen / Esc

Printer-friendly Version

Interactive Discussion



⁸INRA, UMR 1391 ISPA, 33140 Villenave d'Ornon, France

Received: 6 July 2015 – Accepted: 7 July 2015 – Published: 30 July 2015

Correspondence to: G. Boulet (gilles.boulet@ird.fr)

Published by Copernicus Publications on behalf of the European Geosciences Union.

HESSD

12, 7127–7178, 2015

SPARSE model for the prediction of evapotranspiration from TIR data

G. Boulet et al.

Title Page

Abstract

Introduction

Conclusions

References

Tables

Figures



Back

Close

Full Screen / Esc

Printer-friendly Version

Interactive Discussion



and heat fluxes, even if the vegetation is seen as a single “big leaf” and the soil a single “big pore” (Kustas et al., 1996). This is especially true for sparse vegetation, when commonly used scalar profiles within the canopy no longer apply. It also avoids the use of a parameterized kB^{-1} (Kustas and Anderson, 2009).

Beyond evapotranspiration, estimating water stress is also important to infer the surface water status and the root zone soil moisture level (Hain et al., 2009). Water stress can be obtained for the surface as a whole by combining the simulated latent heat flux and the potential latent heat flux, i.e. the theoretical value of the latent heat in current climatic conditions if the surface was still undergoing stage one (unstressed) evapotranspiration (Lhomme, 1997). Dual-source energy balance models allow deriving a rough estimate of the water stress but of the vegetation instead of a soil–vegetation composite. Such frameworks use as input data either the component surface temperatures (e.g. soil and vegetation components retrieved from directional surface temperature data, Jia et al., 2003 or Colaizzi et al., 2012) or a single soil–vegetation composite surface skin temperature. For the former, there is no current operational satellite that offers estimates of temperatures at two contrasted view angles with a very small interval between both acquisitions. For the latter, the TSEB model proposes a realistic underlying assumption to downsize the number of unknowns from two (evaporation E and transpiration T) to one (E or T , Norman et al., 1995). The TSEB model assumes that in most eco- or agro-systems vegetation has access to enough water in the root zone to transpire at a potential rate, so that a modeled potential transpiration rate is a valid first guess estimate for T . This assumption implies that, if vegetation stress is not properly taken into account, the resulting evaporation will decrease to unrealistic levels (negative fluxes) in order to maintain the same total surface temperature, so that a retrieved negative evaporation is a good witness of plant water stress. This assumption is sometimes misleading, and we propose to study its limits.

The original version of TSEB (Norman et al., 1995) provides two algorithms to describe the soil–vegetation–atmosphere interactions, representing respectively the

HESSD

12, 7127–7178, 2015

SPARSE model for the prediction of evapotranspiration from TIR data

G. Boulet et al.

Title Page

Abstract

Introduction

Conclusions

References

Tables

Figures

◀

▶

◀

▶

Back

Close

Full Screen / Esc

Printer-friendly Version

Interactive Discussion



HESSD

12, 7127–7178, 2015

SPARSE model for the prediction of evapotranspiration from TIR data

G. Boulet et al.

Title Page

Abstract

Introduction

Conclusions

References

Tables

Figures

⏪

⏩

◀

▶

Back

Close

Full Screen / Esc

Printer-friendly Version

Interactive Discussion



“patch” and the “layer” approaches following the terminology proposed by Lhomme et al. (2012). In the “layer” approach, one assumes that the air is well mixed within the canopy space so that air temperature at the aerodynamic level is rather homogeneous. The vegetation layer completely covers the ground and prevents the soil from interacting directly (in terms of radiation and turbulent heat transfer) with the atmospheric reference level: soil and vegetation heat sources are fully coupled through a resistance network organized in series (Fig. 1). In the “patch” approach, soil and canopy sources are located side by side, and the soil interacts directly with the air above the canopy. There is a possible lateral gradient in air temperature around the aerodynamic level even though heat transfer around the canopy is associated to the same momentum transfer: soil and vegetation heat sources are thermally uncoupled and fluxes are computed with two parallel resistance schemes. In the original TSEB version, total net radiation is split into soil and vegetation components according to a simple Beer–Lambert law. Several improvements have been proposed later on and implemented in various TSEB versions. Amongst them, one can mention the development of a more complex net radiation scheme, with an initialization of soil and vegetation temperatures in separate formulations of the net radiation of the soil and the canopy (Kustas and Norman, 1999) or the use of an incremental decrease of a transpiration efficiency instead of a bulk retrieval of the latent heat of the vegetation (it corresponds roughly to the ratio between the actual and the potential transpiration rates and matches the definition of the efficiency used in the present work). The TSEB rationale has been translated into several algorithms, with the possibility of using directional radiative temperatures (Kustas and Norman, 1997), day-night temperature difference (Guzinski et al., 2013; Norman et al., 2000), correcting for clumping effects in sparsely vegetated areas (Anderson et al., 2005), and finally by taking into account a Penman–Monteith formulation for potential transpiration (Colaizzi et al., 2012).

Here, we propose to revisit the “layer/series” and “patch/parallel” formulations in order to build a new model based on the same rationale that provides the foundation for all TSEB model versions.

SPARSE model for the prediction of evapotranspiration from TIR data

G. Boulet et al.

[Title Page](#)[Abstract](#)[Introduction](#)[Conclusions](#)[References](#)[Tables](#)[Figures](#)[Back](#)[Close](#)[Full Screen / Esc](#)[Printer-friendly Version](#)[Interactive Discussion](#)

First, we build on the statement by Colaizzi et al. (2012) that, in semi-arid lands, it is more relevant to use a classical resistance scheme instead of the Priestley–Taylor equation, so that adiabatic exchanges are explicitly described. The most common value of the Priestley–Taylor coefficient (close to 1.3) has indeed been challenged for natural vegetation and sites with strong vapour pressure deficit values where root zone moisture is not limiting transpiration (Agam et al., 2010). According to Colaizzi et al. (2014), potential transpiration using Penman–Monteith equation showed better performances compared to the Priestley–Taylor equation. In particular, these authors showed a consistent underestimation of T and overestimation of E when using Priestley–Taylor formulation with the classical 1.3 coefficient, even if total evapotranspiration was similar for both models.

Second, since in the layer approach the vegetation is a semi-infinite cover overlaying the ground, it appears more consistent that this version of the model takes into account not only the soil–vegetation interactions of the turbulent fluxes, but also of the radiative fluxes. Conversely, in the patch approach there is no radiation exchange between the soil and the vegetation patches. This is achieved for the series model through a multiple reflections description between the soil and the overlaying vegetation cover in order to stick more closely to the patch and layer representations schematized in Fig. 1.

Based on those studies, we propose a generalization of the TSEB model (named SPARSE: Soil Plant Atmosphere and Remote Sensing Evapotranspiration model) as a linearization of the full set of energy budget equations and the Choudhury and Monteith (1988) and Shuttleworth and Gurney (1990) expressions of the aerodynamic resistances. The series model is very close to the soil–plant–atmosphere interface of the SiSPAT model (Braud et al., 1995). The full set of equations can be solved either in prescribed conditions (for example, in fully stressed or potential conditions) to compute transpiration and evaporation rates for given stress levels, or in retrieval mode, identically to TSEB. In that case, stress levels are deduced from a known (observed) surface temperature. We propose a third improvement to the existing TSEB model versions, which is similar to what is done in a post-processing step in the single-

source SEBS model (Su, 2002). It consists in bounding each retrieved individual flux component (T , E) by its corresponding potential level deduced from running the model in prescribed potential conditions.

The main objective of the paper is twofold:

1. To describe the SPARSE model, evaluate it against in-situ data and compare its performance with those of the “patch/parallel” and “layer/series” TSEB model formulations, with a focus on the potential gain in robustness obtained when limiting evaporation and transpiration outputs by their corresponding potential rates.
2. Test the retrieval capacities of both “patch/parallel” and “layer/series” versions of the model, not only for total evapotranspiration as well as its components (soil evaporation and transpiration) but also for water stress, first with synthetic data (simulation experiment) and second with in-situ data collected over two wheat fields in semi-arid climate, one irrigated and one rainfed. The purpose of the simulation experiment is specifically to test the limits of the underlying first guess assumptions of TSEB and SPARSE.

2 Series and parallel versions of the SPARSE model

2.1 SPARSE system of equations

The SPARSE model computes the equilibrium surface temperatures of the soil and the vegetation at the meteorological time step as a signature of the energy budget equations of each source. Five main equations are solved simultaneously. The first two represent the energy budget of the soil and the vegetation, the third and the fourth express the continuity (series version) or the summation (parallel version) of the latent and sensible heat fluxes from the soil and the canopy to the aerodynamic level and

SPARSE model for the prediction of evapotranspiration from TIR data

G. Boulet et al.

Title Page

Abstract

Introduction

Conclusions

References

Tables

Figures



Back

Close

Full Screen / Esc

Printer-friendly Version

Interactive Discussion



above, and the fifth describes the link between the radiative surface temperature and its two component temperature sources (soil and vegetation).

Two versions are derived, which can be regarded as fully coupled (series) and fully uncoupled (parallel) soil–vegetation–air exchanges (Fig. 1). This corresponds to (respectively) the “layer” and “patch” approaches described in Lhomme et al. (2012). However, the interpretation of the situations for which one or the other approach is valid differs between TSEB and Lhomme et al. (2012). In TSEB, both soil and vegetation patches share a common surface boundary layer (and therefore the same aerodynamic resistance from the aerodynamic level to the reference level) but the patch representation allows defining different aerodynamic temperatures at the aerodynamic level over the soil and the vegetation. As pointed out by Lhomme et al. (2012), the patch representation should in theory only apply to patches large enough to develop different surface boundary layers, e.g. fallow fields amongst wetter and taller vegetated areas rather than bare soil patches even few meters large. Here, we keep the TSEB assumption for our parallel version and assume that the wind profile in the canopy and above the soil surface are identical in both versions. The main difference lies therefore in the lateral gradient in aerodynamic temperature: in the series version, a single aerodynamic temperature is computed, while in the parallel version two different aerodynamic temperatures are computed above the soil and the canopy, allowing a small departure of the temperature profiles above the soil and the canopy level from the standard mean profile.

The various aerodynamic resistances are computed according to Choudhury and Monteith (1988), Shuttleworth (1985) and Shuttleworth and Gurney (1990) while the stomatal resistance is modelled according to Braud et al. (1995) for all environmental control factors except water stress which is replaced by a transpiration efficiency β_v , and the moisture limited evaporation which is governed by an evaporation efficiency β_s (Mahfouf and Noilhan, 1991). Definitions of β_s and β_v are given just below.

HESSD

12, 7127–7178, 2015

SPARSE model for the prediction of evapotranspiration from TIR data

G. Boulet et al.

Title Page

Abstract

Introduction

Conclusions

References

Tables

Figures

⏪

⏩

◀

▶

Back

Close

Full Screen / Esc

Printer-friendly Version

Interactive Discussion



2.1.1 The series model version

In the series model the latent heat flux components for the soil (LE_s) and the vegetation (LE_v) are representative averages for the surface as a whole:

$$LE_s = \frac{\rho c_p}{\gamma} \beta_s \frac{e_{\text{sat}}(T_s) - e_0}{r_{\text{as}}} \quad (1)$$

$$LE_v = \frac{\rho c_p}{\gamma} \beta_v \frac{e_{\text{sat}}(T_v) - e_0}{r_{\text{vv}}} \quad (2)$$

where ρc_p is the product of air density and specific heat, γ the psychrometric constant, r_{as} the soil to aerodynamic level resistance and r_{vv} the minimum total resistance for latent heat exchange between the vegetation and the aerodynamic level (see Appendix A1); $e_{\text{sat}}(T_x)$ is the saturated vapour pressure at temperature T_x (x refers to “s” for soil, “v” for vegetation) and e_0 is the partial pressure of vapour at the aerodynamic level; T_s and T_v are the soil and the vegetation temperatures respectively.

This formulation is different from that of the most common TSEB algorithms which use the Priestley–Taylor relationship to derive a first estimate of LE_v . Efficiencies β_x are functionally equivalent to surface resistances (again, x referring “s” for soil, “v” for vegetation and is left blank for the total evapotranspiration flux). Their range of validity is $[0, 1]$: if $\beta_v = 1$ then the vegetation transpires at potential rate, and if $\beta_s = 1$ the soil evaporation rate is that of a saturated surface, while $\beta_v = 0$ or $\beta_s = 0$ correspond to a non-transpiring or a non-evaporating surface, respectively. Scaling between those extremes depends on the soil moisture content around the root zone (for β_v) or in the top few centimetres (for β_s). Here, β_v/r_{vv} represents a total canopy resistance including stomatal processes while β_s/r_{as} corresponds to a total soil evaporation resistance, both in actual conditions. There is no minimum resistance to vapour extraction from the soil porous medium, therefore resistances above the soil are the same for sensible and latent heat transfers.

In order to reduce the computational cost of solving the system for all unknown variables including T_s and T_v , all non-linear expressions are linearized through Taylor expansion around air temperature so that the model can be solved through a simple matrix inversion. This is a requirement if one wants to run the model for a large number of pixels. A non-linear model version using optimization routines of the commercial software Matlab™ has been implemented to check the relevance of the linearization, but its computational cost is of course much higher. Eqs. (1) and (2) are converted to Eqs. (3) and (4):

$$LE_s \approx \frac{\rho c_p}{\gamma} \beta_s \frac{e_{\text{sat}}(T_a) + \Delta(T_s - T_a) - e_0}{r_{\text{as}}} \quad (3)$$

$$LE_v \approx \frac{\rho c_p}{\gamma} \beta_v \frac{e_{\text{sat}}(T_a) + \Delta(T_v - T_a) - e_0}{r_{\text{vv}}} \quad (4)$$

where Δ is the slope of the saturation vapour curve at air temperature T_a .

The only non-linear term that is kept in either version is the dependence of the aerodynamic resistance to the stability correction. The latter depends on the difference between the aerodynamic temperature and the reference air temperature (Richardson number, cf. Appendix A1). Aerodynamic temperature is updated iteratively until convergence.

According to the layer representation in Fig. 1, total fluxes (net radiation, sensible heat flux, latent heat flux, soil heat flux) are computed as the sum of the soil and vegetation components. The continuity of the latent heat flux below and above the aerodynamic level implies:

$$LE = LE_s + LE_v = \frac{\rho c_p}{\gamma} \frac{e_0 - e_a}{r_a} \quad (5)$$

where LE_s is expressed in Eq. (3) and LE_v in Eq. (4).

Continuity of the sensible heat reads:

$$H = H_s + H_v = \rho c_p \frac{T_0 - T_a}{r_a} \quad (6)$$

SPARSE model for the prediction of evapotranspiration from TIR data

G. Boulet et al.

Title Page

Abstract

Introduction

Conclusions

References

Tables

Figures

⏪

⏩

◀

▶

Back

Close

Full Screen / Esc

Printer-friendly Version

Interactive Discussion



where T_0 is the aerodynamic temperature and

$$H_s = \rho c_p \frac{T_s - T_0}{r_{as}} \quad (7)$$

$$H_v = \rho c_p \frac{T_v - T_0}{r_{av}} \quad (8)$$

(r_a and r_{av} are the aerodynamic level to reference level and vegetation to aerodynamic level aerodynamic resistances, resp., see Appendix A1 for their complete expression.)

Net radiation depends on the greybody emissions of the soil and vegetation surfaces at temperature T_s and T_v . Taylor expansion for those emission terms in the net radiation estimates leads to:

$$\sigma T_x^4 \approx \sigma T_a^4 + \rho c_p \frac{4\sigma T_a^3}{\rho c_p} (T_x - T_a) = \sigma T_a^4 + \rho c_p \frac{T_x - T_a}{r_{rad}} \quad (9)$$

where σ is the Stefan–Boltzman constant and r_{rad} represents a “radiative resistance”.

Net radiation is computed according to the radiative transfer scheme of Merlin and Chehbouni (2004) which takes into account the multiple reflections between the soil and the vegetation layer in the shortwave and the longwave domains. Application of Eq. (9) on the various equations of this scheme leads to a forcing term depending on the incoming shortwave and longwave radiations, A_x , and a linear expression of the unknown surface temperatures T_s and T_v divided by the appropriate radiative resistances r_{radx} (for the expression of those terms, see Appendix A2). For the soil, this leads to:

$$R_{ns} = A_{ss} - \rho c_p \frac{T_s - T_a}{r_{radss}} - \rho c_p \frac{T_v - T_a}{r_{radsv}} \quad (10)$$

and for the canopy:

$$R_{nv} = A_{vv} - \rho c_p \frac{T_s - T_a}{r_{radvs}} - \rho c_p \frac{T_v - T_a}{r_{radv}} \quad (11)$$

Title Page

Abstract

Introduction

Conclusions

References

Tables

Figures

⏪

⏩

◀

▶

Back

Close

Full Screen / Esc

Printer-friendly Version

Interactive Discussion



The total flux is:

$$R_n = R_{ns} + R_{nv} \quad (12)$$

The soil heat flux G is a fraction ξ of the net radiation available for the whole the soil surface ($G = \xi R_{ns}$). If the model is run at the same time of the day, for instance with surface temperatures acquired with a sun-synchronous satellite, ξ depends mostly on the bare soil fraction cover. For diurnal variations of G , a time-dependent expression (e.g. Santanello and Friedl, 2003) should be preferred.

The resulting energy balance for the soil ($R_{ns} - G = H_s + LE_s$) and the canopy ($R_{nv} = H_v + LE_v$) for the series model can be written as follows:

$$(1 - \xi)A_{ss} = (1 - \xi)\rho c_p \frac{T_s - T_a}{r_{radss}} + (1 - \xi)\rho c_p \frac{T_v - T_a}{r_{radsv}} + \rho c_p \frac{T_s - T_0}{r_{as}} + \frac{\rho c_p}{\gamma} \beta_s \frac{e_{sat}(T_a) + \Delta(T_s - T_a) - e_0}{r_{as}} \quad (13)$$

for the soil and

$$A_{vv} = \rho c_p \frac{T_s - T_a}{r_{radvs}} + \rho c_p \frac{T_v - T_a}{r_{radvv}} + \rho c_p \frac{T_v - T_0}{r_{av}} + \frac{\rho c_p}{\gamma} \beta_v \frac{e_{sat}(T_a) + \Delta(T_v - T_a) - e_0}{r_{vv}} \quad (14)$$

for the vegetation.

Finally, the link between the radiative surface temperature T_{rad} and the net longwave radiation components is:

$$\sigma T_{rad}^4 = R_{atm} - R_{an} \quad (15)$$

where R_{atm} is the incoming atmospheric radiation and R_{an} is the net longwave radiation of the whole surface, which depends on T_s and T_v and can be expressed as follows:

$$R_{an} = A_{atm} - \rho c_p \left(\frac{1}{r_{radss}} + \frac{1}{r_{radvs}} \right) (T_s - T_a) - \rho c_p \left(\frac{1}{r_{radvv}} + \frac{1}{r_{radsv}} \right) (T_v - T_a) \quad (16)$$

The forcing term for the net longwave radiation A_{atm} is given in Appendix A2.

The equation relating the radiative surface temperature T_{rad} and the surface temperatures T_s and T_v is thus:

$$\sigma T_{\text{rad}}^4 + A_{\text{atm}} - R_{\text{atm}} = \rho c_p \left(\frac{1}{r_{\text{radss}}} + \frac{1}{r_{\text{radvs}}} \right) (T_s - T_a) + \rho c_p \left(\frac{1}{r_{\text{radvv}}} + \frac{1}{r_{\text{radsv}}} \right) (T_v - T_a) \quad (17)$$

2.1.2 The parallel model version

For the parallel model, all fluxes are representative of each patch (Fig. 1). The total resistance is the sum of the aerodynamic resistance r_a and the surface resistances r_{as} (for the soil) or r_{vv} (for the canopy). The transpiration rate of the vegetated subpixel (in W m^{-2}) is thus:

$$\text{LE}_v = \frac{\rho c_p}{\gamma} \beta_v \frac{e_{\text{sat}}(T_v) - e_a}{r_{\text{vv}} + r_a} \quad (18)$$

while for the separate patch of bare soil the evaporation rate is:

$$\text{LE}_s = \frac{\rho c_p}{\gamma} \beta_s \frac{e_{\text{sat}}(T_s) - e_a}{r_{\text{as}} + r_a} \quad (19)$$

After linearization, we have:

$$\text{LE}_s \approx \frac{\rho c_p}{\gamma} \beta_s \frac{D_a + \Delta(T_s - T_a)}{r_{\text{as}} + r_a} \quad (20)$$

$$\text{LE}_v \approx \frac{\rho c_p}{\gamma} \beta_v \frac{D_a + \Delta(T_v - T_a)}{r_{\text{vv}} + r_a} \quad (21)$$

where $D_a = e_{\text{sat}}(T_a) - e_a$ is the vapour pressure deficit at reference level. For the parallel model, the sensible heat flux rate and the related continuity of the flux through the aerodynamic level above each patch leads to the following equations:

$$H_s = \rho c_p \frac{T_s - T_a}{r_{\text{as}} + r_a} = \rho c_p \frac{T_s - T_{0s}}{r_{\text{as}}} \quad (22)$$

for the soil, and

$$H_v = \rho c_p \frac{T_v - T_a}{r_{av} + r_a} = \rho c_p \frac{T_v - T_{0v}}{r_{av}} \quad (23)$$

for the vegetation, where T_{0s} is the aerodynamic temperature above the soil and T_{0v} is the aerodynamic temperature above the canopy.

In the parallel model, fluxes from the soil and the vegetation components are computed independently except again for the stability correction for the transfer resistance between the aerodynamic level and the reference level, which depends on an average aerodynamic temperature computed as a weighted average of T_{0s} and T_{0v} :

$$T_0 = (1 - f_c)T_{0s} + f_c T_{0v} \quad (24)$$

Values of T_{0s} and T_{0v} can be derived from Eqs. (22) and (23) once T_s and T_v are known. The value of the leaf area index used for the parallel model is a ‘‘clump LAI’’ obtained by dividing the total LAI by the fraction cover of the vegetation f_c (Lhomme and Chehbouni, 1999). Total fluxes are the sum of the soil and vegetation components also weighted by their relative contribution, f_c for the vegetation and $1 - f_c$ for the soil:

$$LE = (1 - f_c)LE_s + f_c LE_v \quad (25)$$

where LE_s is expressed according to Eq. (20) and LE_v to Eq. (21), and

$$H = (1 - f_c)H_s + f_c H_v \quad (26)$$

where H_s is expressed according to Eq. (22) and H_v to Eq. (23).

For the parallel model, incoming solar and atmospheric radiations are fully available for each source. The net radiation components are solved independently and, like the turbulent fluxes, summed according to their respective cover fraction. The radiative

SPARSE model for the prediction of evapotranspiration from TIR data

G. Boulet et al.

Title Page

Abstract

Introduction

Conclusions

References

Tables

Figures

◀

▶

◀

▶

Back

Close

Full Screen / Esc

Printer-friendly Version

Interactive Discussion



transfer scheme is simpler than for the series model. The Taylor expansion of the net radiation expression for the soil writes:

$$R_{ns} = A_s - \rho c_p \frac{T_s - T_a}{r_{rads}} \quad (27)$$

and for the vegetation:

$$R_{nv} = A_v - \rho c_p \frac{T_v - T_a}{r_{radv}} \quad (28)$$

where A_s and A_v are the radiation forcing terms for the soil and the vegetation, respectively (see Appendix A2 for their numerical expression).

The total flux is:

$$R_n = (1 - f_c)R_{ns} + f_c R_{nv} \quad (29)$$

The soil heat flux G is a fraction ξ of the net radiation available on the bare soil patch ($G = (1 - f_c)\xi R_{ns}$).

Finally, the respective energy balance equations for the soil and the vegetation patches of the parallel model are:

$$(1 - \xi)A_s = (1 - \xi)\rho c_p \frac{T_s - T_a}{r_{rads}} + \rho c_p \frac{T_s - T_a}{r_{as} + r_a} + \frac{\rho c_p}{\gamma} \beta_s \frac{D_a + \Delta(T_s - T_a)}{r_{as} + r_a} \quad (30)$$

and

$$A_v = \rho c_p \frac{T_v - T_a}{r_{radv}} + \rho c_p \frac{T_v - T_a}{r_{av} + r_a} + \frac{\rho c_p}{\gamma} \beta_v \frac{D_a + \Delta(T_v - T_a)}{r_{vw} + r_a} \quad (31)$$

For the parallel version, the net longwave radiation has also a simpler expression than for the series model:

$$R_{an} = (1 - f_c) \left[\varepsilon_s \left(R_{atm} - \sigma T_a^4 \right) - \rho c_p \frac{T_s - T_a}{r_{rads}} \right] + f_c \left[\varepsilon_v \left(R_{atm} - \sigma T_a^4 \right) - \rho c_p \frac{T_v - T_a}{r_{radv}} \right] \quad (32)$$

HESSD

12, 7127–7178, 2015

SPARSE model for the prediction of evapotranspiration from TIR data

G. Boulet et al.

Title Page

Abstract

Introduction

Conclusions

References

Tables

Figures

⏪

⏩

◀

▶

Back

Close

Full Screen / Esc

Printer-friendly Version

Interactive Discussion



The equation relating the radiative surface temperature T_{rad} and the surface temperatures T_s and T_v is thus:

$$\sigma T_{\text{rad}}^4 - R_{\text{atm}} + \left[(1 - f_c)\epsilon_s + f_c\epsilon_v \right] \left[R_{\text{atm}} - \sigma T_a^4 \right] = (1 - f_c)\rho c_p \frac{T_s - T_a}{r_{\text{rads}}} + f_c\rho c_p \frac{T_v - T_a}{r_{\text{radv}}} \quad (33)$$

2.2 “Prescribed” and “retrieval” modes

The system of five equations to be solved simultaneously consists in Eqs. (5), (6), (13), (14) and (17) for the series model, and Eqs. (25), (26), (30), (31) and (33) for the parallel model. This system can be solved in a forward mode for which the surface temperature is an output, and an inverse mode when the surface temperature is an input. The SPARSE model combines both modes (cf. Fig. 2).

If the soil and the vegetation efficiencies are known (for example through an ancillary two compartments water budget model) then the model is run in a forward mode from prescribed water stress conditions (from fully stressed to potential). In that case the system is solved for the following unknowns: T_{rad} , T_s , T_v , e_0 and T_0 . T_{rad} in this prescribed mode is then an output of the system computed from Eqs. (17) and (33) after solving for T_s , T_v , e_0 and T_0 in the other four equations. This mode has two direct applications. It can be used independently from the retrieval mode to generate an equilibrium surface temperature at the time of the satellite overpass in order to assimilate surface temperature measurements from known β_s and β_v values computed at the daily or subdaily timesteps from a hydrological model (e.g. Er-raki et al., 2008). It is also implemented as a final step in the retrieval mode to provide theoretical limits corresponding to maximum reachable levels of sensible heat (fully stressed conditions) or latent heat (potential conditions) for each component (the soil and the vegetation). Output fluxes from the retrieval run are bounded by those limiting cases. In full potential conditions, $\beta_s = \beta_v = 1$ while in fully stressed conditions $\beta_s = \beta_v = 0$.

In retrieval conditions (inverse mode), T_{rad} is known and is derived from satellite observations or in-situ measurements in the thermal infra red domain. In order to compute the various fluxes of the energy balance, the full set of five equations must be

solved simultaneously by inverting the matrix corresponding to Eqs. (5), (6), (13), (14) and (17) for the series model and Eqs. (25), (26), (30), (31) and (33) for the parallel model. The problem is initially ill-posed since the system contains six unknowns: evaporation LE_s and transpiration LE_v , surface temperature components T_s and T_v , and aerodynamic level conditions e_0 and T_0 . LE_s and LE_v values are directly converted into stress levels β_s and β_v using Eqs. (3) and (4) (series model) or (20) and (21) (parallel model). In order to downsize the number of unknowns, SPARSE carries out the same rationale than the TSEB model: as a first guess, the vegetation is supposed to transpire at potential rate, therefore β_v is set to 1, and the system is solved for unknown LE_s (thus β_s), T_s , T_v , e_0 and T_0 . If a negative LE_s is obtained, then the assumption of an unstressed canopy proves to be inconsistent with the observed surface temperature level. In that case, one assumes that the vegetation is suffering from water stress. This means that root zone soil moisture is depleted under critical levels, and that, most probably, the soil surface is already long dry. Therefore, β_s is set to 0 and the system is solved for LE_v (thus β_v) instead of LE_s . Finally, if LE_v is negative, fully stressed conditions are imposed for both the soil and the vegetation independently from T_{rad} . Of course, inconsistent positive values of LE_s corresponding to slightly stressed vegetation conditions can occur when one assumes that the vegetation is unstressed, but in that case the model won't be able to detect this inconsistency. The limit of this hypothesis will be assessed in Sect. 3 through a synthetic case study.

Finally, in order to ensure that LE_x outputs are within realistic bounds, LE_x values are limited by the evapotranspiration components in potential conditions $LE_x(\beta_s = 1, \beta_v = 1)$ in a similar way to the single-source model SEBS (Su, 2002). The impact of limiting LE_x outputs on the model performance will be assessed in Sect. 4.

Also, an arbitrary minimum positive value of $LE_s = 30 \text{ W m}^{-2}$ is used as the threshold for vegetation stress detection instead of 0, in order to take into account the contribution of vapour transfer from within the topsoil porous network (Boulet et al., 1997).

HESSD

12, 7127–7178, 2015

SPARSE model for the prediction of evapotranspiration from TIR data

G. Boulet et al.

Title Page

Abstract

Introduction

Conclusions

References

Tables

Figures

◀

▶

◀

▶

Back

Close

Full Screen / Esc

Printer-friendly Version

Interactive Discussion



3 Assessing the retrieval properties of SPARSE through a synthetic case study

3.1 Principles of the simulation experiment

The strong underlying assumptions behind SPARSE are (i) in a first guess the vegetation is supposed to be unstressed, and (ii) water stress of the vegetation is always concomitant to a non evaporative soil. This simplification of the soil–vegetation–atmosphere continuum impacts not only the total evapotranspiration retrieval but also its resulting partition between transpiration and soil evaporation. It is thus important to assess the limits of both assumptions. To do so, a synthetic simulation experiment is proposed.

The rationale of the synthetic test is as follows: for each combination of known water stress levels affecting either the transpiration or the evaporation of the soil, one can simulate through the energy budgets of the soil and the vegetation the resulting component temperatures T_s and T_v and the surface temperature of the whole surface (T_{rad}). If one assumes that the satellite is actually measuring this temperature, it can be used as input data to get back to the soil evaporation and transpiration levels and their corresponding efficiencies through the retrieval mode. If there was a unique bijective relationship between the component temperatures and the temperature of the whole surface, the retrieved stress levels would correspond to the exact combination of the stress levels used to generate T_{rad} . Of course this is not the case and many different combinations of soil and vegetation efficiency values will correspond to the same equilibrium surface temperature. However, one expects that the whole surface energy balance is well constrained by the knowledge of T_{rad} , i.e. that each value of T_{rad} corresponds to only one surface stress level (or total efficiency). In other words, we expect that SPARSE will not always partition accurately total ET in E and T , but will retrieve the ET value relatively satisfactorily.

The objective of the synthetic stress is to assess the inconsistencies of the decision tree that distributes acceptable stress values between the soil and the

SPARSE model for the prediction of evapotranspiration from TIR data

G. Boulet et al.

[Title Page](#)[Abstract](#)[Introduction](#)[Conclusions](#)[References](#)[Tables](#)[Figures](#)[◀](#)[▶](#)[◀](#)[▶](#)[Back](#)[Close](#)[Full Screen / Esc](#)[Printer-friendly Version](#)[Interactive Discussion](#)

vegetation, as well as its impact on the component and total evapotranspiration retrieval performances.

3.2 Set-up of the synthetic test

In this simulation experiment, the SPARSE model is run sequentially in its two operating modes: the “prescribed” or “forward” mode to generate an estimate of the radiative surface temperature from prescribed β_s and β_v efficiencies, and the “retrieval” or “inverse” mode to retrieve β_s and β_v efficiencies using as input data the surface temperature obtained previously through the “prescribed” mode (“synthetic test” branch of Fig. 2). The test consists therefore in computing a mixed surface radiative temperature (T_{rad}), soil evaporation (LE_s), transpiration (LE_v) and evapotranspiration (LE) for each possible combination of soil evaporation ($\beta_s \in [0, 1]$) and transpiration ($\beta_v \in [0, 1]$) efficiencies in 0.1 increments with the SPARSE model in prescribed mode, then forcing the SPARSE model with T_{rad} to retrieve new LE_s , LE_v and total evapotranspiration LE values as well as the corresponding efficiencies (β_s , β_v and β for the total). β is deduced as the ratio between two total evapotranspiration estimates: one with actual β_s and β_v and one with $\beta_s = \beta_v = 1$. In order to assess the limits of the model assumptions for each version, the prescribed and the retrieval modes are run for the same version (series or parallel): the surface temperature obtained by each combination of β_s and β_v for the series model (resp. the parallel model) in prescribed conditions is used as input for the series model in retrieval mode (resp. the parallel model). The retrieval performance is then assessed by comparing these new retrieved β_s , β_v and β values and the ones used to generate T_{rad} . If the retrieval is fully consistent, those efficiencies must match. The test is carried out for average dry climate conditions ($R_g = 800 \text{ W m}^{-2}$, $\text{RH} = 50 \%$, $u_a = 2 \text{ m s}^{-1}$, $T_a = 25^\circ \text{C}$) and a Leaf Area Index characteristic of maximum development stage of a cereal cover in dry climates ($\text{LAI} = 3$).

HESSD

12, 7127–7178, 2015

SPARSE model for the prediction of evapotranspiration from TIR data

G. Boulet et al.

Title Page

Abstract

Introduction

Conclusions

References

Tables

Figures

⏪

⏩

◀

▶

Back

Close

Full Screen / Esc

Printer-friendly Version

Interactive Discussion



3.3 Results

Results for the total evapotranspiration efficiency retrieval are illustrated in Fig. 3. One expects rather good performances (albeit some bias) close to the first guess assumptions (transpiration close to potential conditions, i.e. $\beta_v \cong 1$ and low soil evaporation i.e. $\beta_s \cong 0$) with a degradation when soil evaporation is high and transpiration is low. In Fig. 3, retrieved total efficiency is compared to the prescribed total efficiency for various incremental values of β_v for two discrete levels of β_s (0.6 and 0.2, top plots), and for incremental values of β_s for two discrete levels of β_v (0.8 and 0.4, bottom plots).

Total evapotranspiration and its corresponding β efficiency value is well retrieved for each $[\beta_s, \beta_v]$ combination for the series model formulation (blue points all aligned along the $[1 : 1]$ line), while for the parallel model β is reasonably well retrieved for situations close to the model assumptions, i.e. a low β_s and a high β_v . For extreme stress values when the assumption underlying SPARSE algorithms is challenged (low transpiration and non negligible soil evaporation) the parallel model tends to overestimate β .

In Fig. 4, the performance of transpiration (top plots) and evaporation (bottom plots) efficiency retrievals are assessed separately. Since the first guess of SPARSE is that the vegetation is unstressed, the model will tend to overestimate β_v . This is the case for all transpiration efficiency values, with, as expected, a larger difference close to a fully transpiring canopy when the inconsistency in β_s retrieval is not yet detected. Indeed, for β_v values close to 1, the initial guess of an unstressed canopy leads to assign a fix value of 1 to β_v . The vegetation temperature is therefore underestimated, and the soil temperature that matches the total surface radiative temperature is overestimated. In turn, sensible heat over the soil is overestimated, the soil net radiation is underestimated, and the resulting soil evaporation computed as a residual term is underestimated. As long as this underestimation does not lead to a negative value of β_s , the model does not detect the discrepancy. Consequently, especially for a wet soil (top plot on the left hand side, $\beta_s = 0.8$), β_v retrievals match poorly the prescribed

HESSD

12, 7127–7178, 2015

SPARSE model for the prediction of evapotranspiration from TIR data

G. Boulet et al.

Title Page

Abstract

Introduction

Conclusions

References

Tables

Figures

⏪

⏩

◀

▶

Back

Close

Full Screen / Esc

Printer-friendly Version

Interactive Discussion



values, and β_v values cling to the unstressed boundary, except for very high prescribed stress levels (β_v below 0.4 for the series model, 0.2 for the parallel one).

Despite this overestimation, β_v retrievals are relatively consistent if the soil is very dry (top plot on the right hand side, $\beta_s = 0.2$). Once again β_v retrievals by the series model are closer to the prescribed values than those of the parallel model. Conversely, soil evaporation retrievals (bottom plots) show, as expected, a slight underestimation when the vegetation is close to unstressed (left hand plot, $\beta_v = 0.8$). Its amplitude is fairly constant and mirrors the overestimation of the transpiration efficiencies when the soil is dry. In that case, blue dots (series) and red squares (parallel) of the retrievals are close to the [1 : 1] line for all β_s levels.

For conditions far from the initial assumption, e.g. low transpiration efficiencies, soil evaporation is largely underestimated. One must note that this is the case for both models and all β_s values. Again, moderately stressed vegetation and a low level soil evaporation rate will always be interpreted in terms of composite surface temperature as a dry soil and fully transpiring vegetation. As a consequence, very small rain events on an otherwise dry soil will most probably be interpreted as a dry soil surface with slightly stressed vegetation. Those cases, not very frequent but not rare either, must be treated with care in a data assimilation perspective.

All those biases should be kept in mind when interpreting results from all dual-source models based on the same rationale: the fact that the total flux is well simulated does not always mean that the component fluxes are consistent, let alone realistic. This has been shown for this particular synthetic dataset.

4 Application over irrigated and rainfed wheat

4.1 Datasets

Two datasets were used to assess the performance of the series and parallel versions of the SPARSE model over a whole growing season. The first experimental dataset

HESSD

12, 7127–7178, 2015

SPARSE model for the prediction of evapotranspiration from TIR data

G. Boulet et al.

Title Page

Abstract

Introduction

Conclusions

References

Tables

Figures

⏪

⏩

◀

▶

Back

Close

Full Screen / Esc

Printer-friendly Version

Interactive Discussion



**SPARSE model for
the prediction of
evapotranspiration
from TIR data**

G. Boulet et al.

[Title Page](#)[Abstract](#)[Introduction](#)[Conclusions](#)[References](#)[Tables](#)[Figures](#)[⏪](#)[⏩](#)[◀](#)[▶](#)[Back](#)[Close](#)[Full Screen / Esc](#)[Printer-friendly Version](#)[Interactive Discussion](#)

was collected over a rainfed wheat with green leaf area index values up to 2 and the second over an irrigated wheat with green LAI up to 4. Both have been grown in a semi-arid climate (central Tunisia and Morocco). Surface temperature data were acquired with an Apogee thermoradiometer, while energy fluxes were measured according to classical FLUXNET recommendations (Baldocchi et al., 2001) with Campbell™ CSAT sonic anemometers and Krypton fast response hygrometers. Observed and simulated latent heat flux values (half hourly averages in W m^{-2}) are compared at midday (local standard time) in all sky conditions. Bowen ratio and the residual method have been used to close the energy balance for the irrigated and rainfed wheat sites, respectively, due to the fast response hygrometer failures of the latter site. Data for the irrigated wheat site have been acquired during the 2004 growing season (B124 site, Boulet et al., 2012), while the experiment for the rainfed wheat took place in 2012.

Leaf area index was estimated with hemispherical photography every 2–3 weeks depending on the phenological cycle, validated by destructive measurements during key stages (growth and full cover). Vegetation height was measured at the same dates. Temporal interpolation of leaf area index for both sites is shown in Fig. 5.

4.2 Evapotranspiration estimates

Two sets of simulations are derived for each model version (series or parallel): in the set the most faithful to the original TSEB, outputs are not limited by potential heat flux values; in the second set, outputs are, like in SEBS, bounded by the potential and fully stressed flux rates considered at absolute maximum and minimum reachable values for evaporation as well as transpiration, whatever the “oasis” or micro-advection heat transfer might be. Again, this is legitimate for the parallel version, but for the series version one must inquire if local advection effects do not enhance latent heat flux values over the total potential value of a uniformly wet surface. No calibration is performed, the minimum stomatal resistance value is arbitrarily set to a realistic level for herbaceous vegetation (100 s m^{-1}) and the G/R_{ns} ratio ξ is set to 40% (value often encountered around midday for bare soils in arid climates). This is consistent with the potential use of

this model which is designed to estimate ET routinely from remote sensing data, based on surface properties derived per land use type in a similar way to most SVATs applied to continental scales. Those values are of course less sensitive than the uncertainty on the input variable T_{rad} (not shown).

Total flux values are shown in Figs. 6 and 7 for the bounded sets and RMSE values for both bounded and unbounded sets are reported in Table 1. In both cases (series and parallel versions) the RMSE values are almost similar and consistent with values found in the literature (cf. Li et al., 2005). The bounded series outputs display the best performances, with RMSE values lowered by 4 to more than 10 W m^{-2} . RMSE values for the parallel TSEB version of Kustas et al. (1999) are very close to that of the SPARSE parallel version while RMSE values for the TSEB series model built from Cammalleri et al. (2010) are similar to the RMSE values displayed by both parallel versions.

Retrieval performances of the other energy balance components in the bounded case have also been assessed. Statistics are shown in Table 2. The series model shows slightly better retrieval performances for soil heat flux for both sites, but only for net radiation for the irrigated wheat and for sensible heat for the rainfed wheat site. This is consistent with Li et al. (2005) and Morillas et al. (2013).

4.3 Water stress estimates

Low RMSE values for the total latent heat flux do not warranty that total water stress is correctly simulated. Indeed, if moisture availability in the root zone is large enough to maintain ET at potential levels, the prescribed model in potential conditions can already explain a very large amount of the information content within the observed time series, and the added value of TIR data might be limited. It is thus important to assess the amount of information introduced by the surface temperature itself, i.e. information on moisture limited evaporation and transpiration rates (i.e. second stage evaporation, cf. Boulet et al., 2004). Water stress is usually defined as the complementary part to 1 of the ratio between the actual and the potential evapotranspiration rates. It

HESSD

12, 7127–7178, 2015

SPARSE model for the prediction of evapotranspiration from TIR data

G. Boulet et al.

Title Page

Abstract

Introduction

Conclusions

References

Tables

Figures



Back

Close

Full Screen / Esc

Printer-friendly Version

Interactive Discussion



is expected to scale between 0 (unstressed surface) and 1 (fully stressed surface). Retrieved and observed surface water stress values have been estimated from potential evapotranspiration rates generated with the SPARSE model in prescribed conditions ($\beta_s = \beta_v = 1$). Simulated and observed water stress values are computed as $1 - LE/LE_p$ and $1 - LE_{obs}/LE_p$ respectively, where LE_{obs} is the instantaneous observed latent heat flux while LE and LE_p are the simulated latent heat flux in actual and potential conditions respectively. Total stress is thus functionally equivalent to $1 - \beta$. Results are shown in Figs. 8 and 9. As expected, surface stress is much higher for the rainfed than for the irrigated wheat field. The scatter is quite large, therefore showing the intrinsic limit of stress retrieval from naturally noisy TIR data as already pointed out by numerous studies (Gentine et al., 2010; Katul et al., 1998; Lagouarde et al., 2013, 2015). However, broad tendencies are well reproduced, with most points located within a confidence interval of 0.2 indicated by dotted lines along the 1 : 1 line. This is encouraging in a data assimilation perspective. One must also note that it includes small LE and LE_p values for which measurement uncertainty can be as large as the flux itself. To scale those stress values back to potential evapotranspiration, the LE_p order of magnitude is indicated as marker size in Figs. 8 and 9. Most outliers have smaller LE_p values while the points with the largest LE_p fall within the space delimited by the two dotted lines of the confidence interval.

Some points with little to no evaporation attest the difficulty to represent accurately the conditions close to the potential levels and might be related to the theoretical limit of the model for small vegetation stress values illustrated in Fig. 3, especially at low evaporation efficiencies.

4.4 Soil evaporation efficiency

As shown in the previous sections as well as many previous studies on soil–vegetation–atmosphere interactions in the literature (Li et al., 2005; Morillas et al., 2013), series and parallel versions have fairly similar performances in total flux retrieval even though the series version shows slightly better values for the selected statistical criterion.

SPARSE model for the prediction of evapotranspiration from TIR data

G. Boulet et al.

Title Page

Abstract

Introduction

Conclusions

References

Tables

Figures



Back

Close

Full Screen / Esc

Printer-friendly Version

Interactive Discussion



HESSD

12, 7127–7178, 2015

SPARSE model for the prediction of evapotranspiration from TIR data

G. Boulet et al.

Title Page

Abstract

Introduction

Conclusions

References

Tables

Figures

⏪

⏩

◀

▶

Back

Close

Full Screen / Esc

Printer-friendly Version

Interactive Discussion



However, as illustrated with the synthetic case, it might not be the case for component flux retrieval. In order to check the consistency of component flux retrieval, one needs a measurement of either soil evaporation or transpiration. In neither sites transpiration data have been collected: measuring transpiration for a cereal cover is quite challenging. On the other hand, surface soil moisture data (at a depth of around 5 cm) are available at both sites. Of course, soil moisture at 5 cm does not always react to small rainfall events, but it is a good driver of soil evaporation despite its influence by shallow roots.

We therefore decided to compare the retrieved soil evaporation efficiency to a fairly independent evaluation noted β_{s_e} derived from the observed time series of soil moisture in the top 5 cm ($\theta_{0-5\text{cm}}$) instead of using TIR data. We used the efficiency model of Merlin et al. (2011) to derive β_{s_e} :

$$\beta_{s_e} = \left[0.5 - 0.5 \cos \left(\pi \frac{\theta_{0-5\text{cm}}}{\theta_{\text{sat}}} \right) \right]^p \quad (34)$$

Where θ_{sat} is the water content at saturation and p is fixed to 1 for the loamy site (rainfed wheat) and 0.5 for the clay site (irrigated wheat) according to $1 - LE/LE_p$ observations at the beginning and the end of the growing season when the soil is almost bare.

Since the surface temperature (and thus the partition between LE_s and LE_v) reacts immediately to atmospheric turbulence (Lagouarde et al., 2015) or very small rainfall events, β_s instantaneous retrievals by SPARSE show larger fluctuations than β_{s_e} . Indeed, the latter reacts mostly to the largest rainfall events (wetting of the entire 5 cm topsoil). Meteorological forcing can vary quickly and impact the potential soil evaporation rate LE_{sp} , but the latter is less sensitive to turbulence than T_{rad} . In order to smooth out the quick fluctuations of β_s retrievals by SPARSE, we compare 5 days running averages of β_s and β_{s_e} .

The resulting β_s and β_{s_e} evaporation efficiencies are shown on Figs. 10 (rainfed wheat) and 11 (irrigated wheat). For both sites, increasing and decreasing trends of

β_s and β_{s_e} are mostly synchronous, although their amplitude varies throughout the growing season. Due to irrigation, β_s values are on average higher for the irrigated than the rainfed wheat site.

For the rainfed site, both models simulate fairly large values of β_s compared to β_{s_e} at the beginning of the season. The parallel model agrees well with β_{s_e} towards the end of the growing stage (DOY 30–70) while the series model matches very closely β_{s_e} at maximum cover and early senescence (reduction of β_s from DOY 70 to DOY 100). Both models agree well with β_{s_e} at the end of the season (DOY 120–170) except for the last ten days. The small rainfall event around DOY 125 is not sufficient to impact β_{s_e} but affects β_s in both model versions, whereas the soil moisture increase around DOY 105 is mostly missed out by either version.

For the irrigated wheat, soil evaporation is mostly in the energy limited stage for the first half of the observation period, and β_s remains close to 1. This is due to the complement irrigation up to the middle of the maturation phase. The magnitude of both drying events around DOY 40 and DOY 100 is very well retrieved by the series model and somewhat less by the parallel model. Again, β_s reacts more strongly to the small rainfall event around DOY 90 than what is indicated from soil moisture.

At the very end of the season both model versions differ greatly from the β_{s_e} estimates and remain close to the potential rate for both sites.

5 Discussion and conclusion

A new model based on the TSEB rationale, SPARSE, has been presented. Innovation lies mostly in the formulation of the energy balance equations and the use of complementary modes (prescribed and retrieval) which allow to bound the outputs by realistic limiting flux values which ensure increased robustness. We demonstrated with two datasets that using bounding relationships based on potential conditions decreases the root mean square error by up to 11 W m^{-2} from values of the order of $50\text{--}80 \text{ W m}^{-2}$. Theoretical limitations of the performance of the evapotranspiration

HESSD

12, 7127–7178, 2015

SPARSE model for the prediction of evapotranspiration from TIR data

G. Boulet et al.

Title Page

Abstract

Introduction

Conclusions

References

Tables

Figures

⏪

⏩

⏴

⏵

Back

Close

Full Screen / Esc

Printer-friendly Version

Interactive Discussion



SPARSE model for the prediction of evapotranspiration from TIR dataG. Boulet et al.

[Title Page](#)[Abstract](#)[Introduction](#)[Conclusions](#)[References](#)[Tables](#)[Figures](#)[Back](#)[Close](#)[Full Screen / Esc](#)[Printer-friendly Version](#)[Interactive Discussion](#)

components (evaporation and transpiration) retrievals from a single radiative surface temperature have been inferred over rainfed and irrigated wheat fields at seasonal scales, as well as through a theoretical simulation exercise. For very high vegetation stress levels it is almost impossible to retrieve a non-zero soil evaporation at medium to large LAI values. Also, and by construction, transpiration tends to be overestimated in most ranges but specifically when only slightly stressed. Within these limits, the SPARSE model shows good retrieval performances of evapotranspiration compared to the original TSEB. As expected for cereal covers whose homogeneity is usually well represented by a “layer” approach, the series version provides in general better estimates in both real and synthetic cases tested. Those cases are representative of cereals typically grown in semi-arid lands in irrigated and non-irrigated areas. Both models should be tested for other conditions of heterogeneity (sparse crops, orchards, row crops) whose geometrical features are closer to the “patch” description.

Estimates of water stress have also been looked at. Water stress is an interesting variable that can be assimilated in all hydrological or SVAT models in order to compute moisture-limited evapotranspiration rates. Even if the points in the simulated vs. observed scatterplots have a significant number of outliers, i.e. points outside the 0.1 range along the 1 : 1 line in Figs. 8 and 9, the results indicate that the information retrieved from TIR data is useful in a data-assimilation perspective since the broad tendencies are well reproduced.

Estimates of soil evaporation efficiency have been evaluated against a reconstructed time series relying on observed soil moisture at the soil surface and therefore independent from any surface temperature measurement. This reconstruction is of course model-dependent (Merlin et al., 2011 in our case) and must be considered with care, but despite this we found that both efficiency values are consistent, except at the beginning and the end of the season, partly due to very small rainfall events, but also probably to the poor understanding of turbulence processes over low or senescent vegetation. It seems that the transpiration of the quasi-senescent vegetation encountered at this period of the year is not always well simulated by the model even

SPARSE model for the prediction of evapotranspiration from TIR data

G. Boulet et al.

Title Page

Abstract

Introduction

Conclusions

References

Tables

Figures

⏪

⏩

◀

▶

Back

Close

Full Screen / Esc

Printer-friendly Version

Interactive Discussion



if total and green LAI values seem realistic. This could be related to the change in soil–vegetation radiation exchange and drag partition in a drying vegetation with shrinking leaves and standing straw. In order to smooth out the scale differences between the information provided by soil moisture (a time-continuous variable) and that of surface temperature (influenced by high frequency turbulent fluctuations) we compared 5 days moving averages. This is consistent with the potential data assimilation method of β or LE estimated from TIR data that one could use in a SVAT model for example: a smoother is more likely to outperform a sequential assimilation algorithm for short observation windows since the former will naturally smooth-out the high order fluctuations due to high order fluctuations of T_{rad} . Simpler models would perhaps provide similar performances of soil evaporation efficiencies, for instance in rainfed agriculture where surface soil moisture is well constrained by rainfall, but in irrigated areas it is interesting to get proper timing of water inputs and this can be achieved with relatively good confidence with this model provided that TIR information is available frequently enough.

Future work will assess the potential use of microwave data (radar) to infer topsoil moisture and constraint the inversion procedure using a first guess efficiency value generated from topsoil moisture estimates. Current work is directed towards assessing the model performance over other crops, including orchards, and other climates.

Appendix A:

A1 Expression of the various resistances according to Shuttleworth and Gurney (1990)

$$r_a = \frac{\ln\left(\frac{z-d}{z_{om}}\right)^2}{k^2 u_a (1 + Ri)^m}$$

SPARSE model for the prediction of evapotranspiration from TIR data

G. Boulet et al.

[Title Page](#)

[Abstract](#)

[Introduction](#)

[Conclusions](#)

[References](#)

[Tables](#)

[Figures](#)

[⏪](#)

[⏩](#)

[◀](#)

[▶](#)

[Back](#)

[Close](#)

[Full Screen / Esc](#)

[Printer-friendly Version](#)

[Interactive Discussion](#)



$$r_{as} = \frac{z_v e^{n_{SW}} \ln\left(\frac{z-d}{z_{om}}\right) \left(e^{-\frac{n_{SW} z_{om, s}}{z_v}} - e^{-\frac{n_{SW}(d+z_{om})}{z_v}} \right)}{n_{SW} k^2 u_a (z_v - d)}$$

$$r_{av} = \left(\frac{w \ln\left(\frac{z-d}{z_{om}}\right)}{u_a \ln\left(\frac{z_v-d}{z_{om}}\right)} \right)^{0.5} \frac{n_{SW}}{4\alpha_0 LAI (1 - e^{-0.5n_{SW}})}$$

$$r_{vv} = r_{av} + \frac{r_{stmin} \prod f}{LAI}$$

Where u_a is the wind speed measured at height z , z_v the vegetation height, d the displacement height, z_{om} the roughness length for momentum exchange, $n_{SW} = 2.5$, w the width of the leaves (in cm), $\alpha_0 = 0.005$, r_{stmin} the minimum stomatal resistance and $z_{om, s} = 0.005$ m is the roughness length for momentum exchange over bare soil. $Ri = \frac{5g(z-d)(T_0 - T_a)}{T_a u_a^2}$ is the stability correction (Richardson number); $m = 0.75$ in unstable conditions and $m = 2$ in stable conditions. $\prod f$ represent the product of weighting stress functions related to environmental factors affecting the stomatal resistance (temperature, solar radiation, vapour pressure deficit) and are taken from Braud et al. (1995).

A2 Forcing terms and radiative resistances of the net radiation model for the series and the parallel versions of SPARSE

For the series version:

$$A_{ss} = (a_{rads} + b_{rads}) \sigma T_a^4 + c_{rads}$$

$$r_{radss} = -\frac{\rho c_p}{4\sigma T_a^3 a_{rads}}$$

SPARSE model for the prediction of evapotranspiration from TIR data

G. Boulet et al.

Title Page

Abstract

Introduction

Conclusions

References

Tables

Figures

◀

▶

◀

▶

Back

Close

Full Screen / Esc

Printer-friendly Version

Interactive Discussion



$$r_{\text{radsv}} = -\frac{\rho c_p}{b_{\text{rads}} 4\sigma T_a^3}$$

$$A_{\text{VV}} = (a_{\text{radv}} + b_{\text{radv}})\sigma T_a^4 + c_{\text{radv}}$$

$$r_{\text{radvs}} = -\frac{\rho c_p}{a_{\text{radv}} 4\sigma T_a^3}$$

$$r_{\text{radvv}} = -\frac{\rho c_p}{b_{\text{radv}} 4\sigma T_a^3}$$

$$5 \quad A_{\text{atm}} = (a_{\text{rads}} + b_{\text{rads}} + a_{\text{radv}} + b_{\text{radv}})\sigma T_a^4 + c_{\text{ratms}} + c_{\text{ratmv}}$$

where

$$a_{\text{rads}} = -\frac{\varepsilon_s[(1 - f_c) + \varepsilon_v f_c]}{1 - f_c(1 - \varepsilon_s)(1 - \varepsilon_v)}$$

$$b_{\text{rads}} = a_{\text{radv}} = \frac{\varepsilon_v \varepsilon_s f_c}{1 - f_c(1 - \varepsilon_s)(1 - \varepsilon_v)}$$

$$c_{\text{ratms}} = \frac{(1 - f_c)\varepsilon_s R_{\text{atm}}}{1 - f_c(1 - \varepsilon_s)(1 - \varepsilon_v)}$$

$$10 \quad c_{\text{rads}} = \frac{R_g(1 - \alpha_s)(1 - f_c)}{1 - f_c \alpha_s \alpha_v} + c_{\text{ratms}}$$

$$b_{\text{radv}} = -f_c \varepsilon_v \left[1 + \frac{\varepsilon_s + (1 - f_c)(1 - \varepsilon_s)}{1 - f_c(1 - \varepsilon_s)(1 - \varepsilon_v)} \right]$$

$$c_{\text{ratmv}} = f_c \varepsilon_v R_{\text{atm}} \left[1 + \frac{(1 - f_c)(1 - \varepsilon_s)}{1 - f_c(1 - \varepsilon_s)(1 - \varepsilon_v)} \right]$$

$$c_{\text{radv}} = R_g(1 - \alpha_v) f_c \left[1 + \frac{\alpha_s(1 - f_c)}{1 - f_c \alpha_s \alpha_v} \right] + c_{\text{ratmv}}$$

(α_s and ε_s are the albedo and the emissivity of the soil, α_v and ε_v are the albedo and the emissivity of the canopy, and R_g is the global incoming radiation)

For the parallel version:

$$A_s = (1 - \alpha_s)R_g + \varepsilon_s (R_{\text{atm}} - \sigma T_a^4)$$

$$A_v = (1 - \alpha_v)R_g + \varepsilon_v (R_{\text{atm}} - \sigma T_a^4)$$

$$r_{\text{rads}} = \frac{\rho c_p}{4\varepsilon_s \sigma T_a^3}$$

$$r_{\text{radv}} = \frac{\rho c_p}{4\varepsilon_v \sigma T_a^3}$$

Acknowledgements. This work was mostly supported by the French Space Agency (CNES) through TOSCA projects EVA2IRT and EVASPA3. Financial support by ANR for the TRANSMED project AMETHYST (ANR-12-TMED-0006-01) and PHC Maghreb for the project N° 32592VE (“Estimation spatialisée de l’utilisation de l’eau par l’agriculture pluviale et irriguée au Maghreb”) are also gratefully acknowledged. Sustained financial and in kind support by IRD and the MISTRALS (Mediterranean Integrated STudies at Regional And Local Scales) program through its SICMED component is also acknowledged. The authors extend their thanks to the technical teams of IRD, INAT, CTV-Chebika and INGC for their strong collaboration and support for the implementation of ground-truth measurements.

References

- Agam, N., Kustas, W. P., Anderson, M. C., Norman, J. M., Colaizzi, P. D., Howell, T. A., Prueger, J. H., Meyers, T. P., and Wilson, T. B.: Application of the Priestley–Taylor approach in a two-source surface energy balance model, *J. Hydrometeorol.*, 11, 185–198, doi:10.1175/2009jhm1124.1, 2010.
- Amano, E. and Salvucci, G. D.: Detection of three signatures of soil-limited evaporation, *Remote Sens. Environ.*, 67, 108–122, 1997.

SPARSE model for the prediction of evapotranspiration from TIR data

G. Boulet et al.

Title Page

Abstract

Introduction

Conclusions

References

Tables

Figures

⏪

⏩

◀

▶

Back

Close

Full Screen / Esc

Printer-friendly Version

Interactive Discussion



SPARSE model for the prediction of evapotranspiration from TIR data

G. Boulet et al.

[Title Page](#)

[Abstract](#)

[Introduction](#)

[Conclusions](#)

[References](#)

[Tables](#)

[Figures](#)

[⏪](#)

[⏩](#)

[◀](#)

[▶](#)

[Back](#)

[Close](#)

[Full Screen / Esc](#)

[Printer-friendly Version](#)

[Interactive Discussion](#)



Anderson, M. C., Norman, J. M., Kustas, W. P., Li, F., Prueger, J. H., and Mecikalski, J. R.: Effects of vegetation clumping on two-source model estimates of surface energy fluxes from an agricultural landscape during SMACEX, *J. Hydrometeorol.*, 6, 892–909, doi:10.1175/jhm465.1, 2005.

Baldocchi, D., Falge, E., Gu, L., Olson, R., Hollinger, D., Running, S., Anthoni, P., Bernhofer, C., Davis, K., Evans, R., Fuentes, J., Goldstein, A., Katul, G., Law, B., Lee, X., Malhi, Y., Meyers, T., Munger, W., Oechel, W., Paw, K. T., Pilegaard, K., Schmid, H. P., Valentini, R., Verma, S., Vesala, T., Wilson, K., and Wofsy, S.: FLUXNET: a new tool to study the temporal and spatial variability of ecosystem-scale carbon dioxide, water vapor, and energy flux densities, *B. Am. Meteorol. Soc.*, 82, 2415–2434, doi:10.1175/1520-0477(2001)082<2415:fanfts>2.3.co;2, 2001.

Boulet, G., Braud, I., and Vauclin, M.: Study of the mechanisms of evaporation under arid conditions using a detailed model of the soil–atmosphere continuum. Application to the EFEDA I experiment, *J. Hydrol.*, 193, 114–141, 1997.

Boulet, G., Chehbouni, A., Braud, I., Duchemin, B., and Lakhal, A.: Evaluation of a two-stage evaporation approximation for contrasting vegetation cover, *Water Resour. Res.*, 40, W12507, doi:10.1029/2004wr003212, 2004.

Boulet, G., Chehbouni, A., Gentine, P., Duchemin, B., Ezzahar, J., and Hadria, R.: Monitoring water stress using time series of observed to unstressed surface temperature difference, *Agr. Forest Meteorol.*, 146, 159–172, doi:10.1016/j.agrformet.2007.05.012, 2007.

Boulet, G., Olioso, A., Ceschia, E., Marloie, O., Coudert, B., Rivalland, V., Chirouze, J., and Chehbouni, G.: An empirical expression to relate aerodynamic and surface temperatures for use within single-source energy balance models, *Agr. Forest Meteorol.*, 161, 148–155, doi:10.1016/j.agrformet.2012.03.008, 2012.

Braud, I., Dantas-Antonino, A. C., Vauclin, M., Thony, J. L., and Ruelle, P.: A Simple Soil-Plant-Atmosphere Transfer model (SiSPAT), development and field verification, *J. Hydrol.*, 166, 231–260, 1995.

Cammalleri, C., Anderson, M. C., Ciruolo, G., D’Urso, G., Kustas, W. P., La Loggia, G., and Minacapilli, M.: The impact of in-canopy wind profile formulations on heat flux estimation in an open orchard using the remote sensing-based two-source model, *Hydrol. Earth Syst. Sci.*, 14, 2643–2659, doi:10.5194/hess-14-2643-2010, 2010.

**SPARSE model for
the prediction of
evapotranspiration
from TIR data**

G. Boulet et al.

[Title Page](#)[Abstract](#)[Introduction](#)[Conclusions](#)[References](#)[Tables](#)[Figures](#)[⏪](#)[⏩](#)[◀](#)[▶](#)[Back](#)[Close](#)[Full Screen / Esc](#)[Printer-friendly Version](#)[Interactive Discussion](#)

- Lhomme, J.-P.: Towards a rational definition of potential evaporation, *Hydrol. Earth Syst. Sci.*, 1, 257–264, doi:10.5194/hess-1-257-1997, 1997.
- Li, F. Q., Kustas, W. P., Prueger, J. H., Neale, C. M. U., and Jackson, T. J.: Utility of remote sensing-based two-source energy balance model under low- and high-vegetation cover conditions, *J. Hydrometeorol.*, 6, 878–891, 2005.
- 5 Mahfouf, J. and Noilhan, J.: Comparative study of various formulations of evaporations from bare soil using in situ data, *J. Appl. Meteorol.*, 30, 1354–1365, 1991.
- Matsushima, D.: Relations between aerodynamic parameters of heat transfer and thermal-infrared thermometry in the bulk surface formulation, *J. Meteorol. Soc. Jpn.*, 83, 373–389, 2005.
- 10 Merlin, O. and Chehbouni, A.: Different approaches in estimating heat flux using dual angle observations of radiative surface temperature, *Int. J. Remote Sens.*, 25, 275–289, doi:10.1080/0143116031000116408, 2004.
- Merlin, O., Al Bitar, A., Rivalland, V., Beziat, P., Ceschia, E., and Dedieu, G.: An analytical model of evaporation efficiency for unsaturated soil surfaces with an arbitrary thickness, *J. Appl. Meteorol. Clim.*, 50, 457–471, doi:10.1175/2010jamc2418.1, 2011.
- 15 Morillas, L., Garcia, M., Nieto, H., Villagarcia, L., Sandholt, I., Gonzalez-Dugo, M. P., Zarco-Tejada, P. J., and Domingo, F.: Using radiometric surface temperature for surface energy flux estimation in Mediterranean drylands from a two-source perspective, *Remote Sens. Environ.*, 136, 234–246, doi:10.1016/j.rse.2013.05.010, 2013.
- 20 Norman, J. M., Kustas, W. P., and Humes, K. S.: Source approach for estimating soil and vegetation energy fluxes in observations of directional radiometric surface temperature, *Agr. Forest Meteorol.*, 77, 263–293, 1995.
- Norman, J. M., Kustas, W. P., Prueger, J. H., and Diak, G. R.: Surface flux estimation using radiometric temperature: a dual-temperature-difference method to minimize measurement errors, *Water Resour. Res.*, 36, 2263–2274, 2000.
- 25 Olios, A., Inoue, Y., Ortega-Farias, S., Demarty, J., Wigneron, J. P., Braud, I., Jacob, F., Lecharpentier, P., Otlí, C., Calvet, J. C., and Brisson, N.: Future directions for advanced evapotranspiration modeling: assimilation of remote sensing data into crop simulation models and SVAT models, *Irrig. Drain. Systems*, 19, 377–412, 2005.
- 30 Santanello, J. A. and Friedl, M. A.: Diurnal covariation in soil heat flux and net radiation, *J. Appl. Meteorol.*, 42, 851–862, doi:10.1175/1520-0450(2003)042<0851:dcishf>2.0.co;2, 2003.

Shuttleworth, W. J. and Gurney, R. J.: The theoretical relationship between foliage temperature and canopy resistance in sparse crops, Q. J. Roy. Meteor. Soc., 116, 497–519, doi:10.1002/qj.49711649213, 1990.

Shuttleworth, W. J. and Wallace, J. S.: Evaporation from sparse crops - an energy combination theory, Q. J. Roy. Meteor. Soc., 111, 839–855, 1985.

Su, Z.: The Surface Energy Balance System (SEBS) for estimation of turbulent heat fluxes, Hydrol. Earth Syst. Sci., 6, 85–100, doi:10.5194/hess-6-85-2002, 2002.

Verhoef, A., de Bruin, H. A. R., and van den Hurk, B. J. J. M.: Some practical notes on the parameter kB^{-1} for sparse vegetation, J. Appl. Meteorol., 36, 560–572, 1997.

HESSD

12, 7127–7178, 2015

SPARSE model for the prediction of evapotranspiration from TIR data

G. Boulet et al.

Title Page

Abstract

Introduction

Conclusions

References

Tables

Figures

⏪

⏩

◀

▶

Back

Close

Full Screen / Esc

Printer-friendly Version

Interactive Discussion



HESSD

12, 7127–7178, 2015

SPARSE model for the prediction of evapotranspiration from TIR data

G. Boulet et al.

Table 2. Performances of instantaneous retrievals at midday for net radiation, total sensible heat flux and soil heat flux (root mean square error in W m^{-2}); TSEB version is that of Kustas and Norman (1999).

		Rainfed wheat	Irrigated wheat
Net radiation	Series	68	50
	Parallel	60	58
	TSEB	78	61
Sensible Heat Flux	Series	61	74
	Parallel	65	60
	TSEB	76	60
Soil Heat Flux	Series	49	37
	Parallel	53	49
	TSEB	52	44

Title Page

Abstract

Introduction

Conclusions

References

Tables

Figures

⏪

⏩

◀

▶

Back

Close

Full Screen / Esc

Printer-friendly Version

Interactive Discussion



Table A1. Symbols.

a_{rads}	Coefficient in $r_{\text{rads}}, A_{\text{atm}}$ and A_{ss}
a_{radv}	Coefficient in $r_{\text{radvs}}, A_{\text{atm}}$ and A_{vv}
A_{s}	Forcing term of the soil net radiation for the parallel model (W m^{-2})
A_{v}	Forcing term of the vegetation net radiation for the parallel model (W m^{-2})
A_{ss}	Forcing term of the soil net radiation for the series model (W m^{-2})
A_{vv}	Forcing term of the vegetation net radiation for the series model (W m^{-2})
b_{rads}	Coefficient in $r_{\text{rads}}, A_{\text{atm}}$ and A_{ss}
b_{radv}	Coefficient in $r_{\text{radsv}}, A_{\text{atm}}$ and A_{vv}
c_p	Specific heat of air at constant pressure ($\text{J kg}^{-1} \text{K}^{-1}$)
c_{rads}	Coefficient in A_{ss}
c_{radv}	Coefficient in A_{vv}
c_{ratms}	Coefficient in A_{atm}
c_{ratmv}	Coefficient in A_{atm}
d	Displacement height (m)
e_a	Air vapour pressure at reference level (Pa)
e_0	Air vapour pressure at the aerodynamic level (Pa)
$e_{\text{sat}}(T_x)$	Saturated vapour pressure at temperature T_x (Pa)
f_c	Vegetation cover fraction
G	Soil heat flux (W m^{-2})
g	Gravitational constant (m s^{-2})
H	Total sensible heat flux (W m^{-2})
H_s	Sensible heat flux from the soil (W m^{-2})
H_v	Sensible heat flux from the canopy (W m^{-2})
LE	Total latent heat flux (W m^{-2})
LE_p	Total latent heat flux in potential conditions (W m^{-2})
LE_s	Latent heat flux from the soil (W m^{-2})
LE_{sp}	Latent heat flux from the soil in potential conditions (W m^{-2})
LE_v	Latent heat flux from the canopy (W m^{-2})
LE_{vp}	Latent heat flux from the canopy in potential conditions (W m^{-2})
m	Coefficient of the stability function (W m^{-2})
n_{sw}	Coefficient in r_{av}
r_a	Aerodynamic resistance between the aerodynamic level and the reference level (s m^{-1})
R_{an}	Longwave net radiation (W m^{-2})
r_{as}	Aerodynamic resistance between the aerodynamic level and the reference level (s m^{-1})
R_{atm}	Incoming atmospheric radiation (W m^{-2})
r_{av}	Aerodynamic resistance between the aerodynamic level and the reference level (s m^{-1})
R_g	Incoming solar radiation (W m^{-2})
Ri	Richardson number

[Title Page](#)

[Abstract](#)

[Introduction](#)

[Conclusions](#)

[References](#)

[Tables](#)

[Figures](#)

[⏪](#)

[⏩](#)

[◀](#)

[▶](#)

[Back](#)

[Close](#)

[Full Screen / Esc](#)

[Printer-friendly Version](#)

[Interactive Discussion](#)



Table A1. Continued.

R_n	Total net radiation ($W m^{-2}$)
R_{ns}	Net radiation over the soil ($W m^{-2}$)
R_{nv}	Net radiation over the canopy ($W m^{-2}$)
r_{rad}	Radiative resistance ($s m^{-1}$)
r_{rads}	Soil radiative resistance for the parallel model ($s m^{-1}$)
r_{radv}	Canopy radiative resistance for the parallel model ($s m^{-1}$)
r_{radss}	Soil radiative resistance for the soil net radiation in the series model ($s m^{-1}$)
r_{radsv}	Canopy radiative resistance for the soil net radiation in the series model ($s m^{-1}$)
r_{radvs}	Soil radiative resistance for the vegetation net radiation in the series model ($s m^{-1}$)
r_{radvv}	Canopy radiative resistance for the vegetation net radiation in the series model ($s m^{-1}$)
r_{stmin}	Minimum stomatal resistance ($s m^{-1}$)
r_{vv}	Surface resistance between the aerodynamic level and the reference level ($s m^{-1}$)
T_0	Aerodynamic temperature
T_{0s}	Aerodynamic temperature over the soil patch
T_{0v}	Aerodynamic temperature over the vegetation patch (K)
T_a	Air temperature at reference level (K)
T_s	Soil surface temperature (K)
T_v	Vegetation surface temperature (K)
u_a	Horizontal wind speed at reference level ($m s^{-1}$)
w	Leaf width (cm)
z	Reference height where air forcing variables are measured (m)
z_{om}	Roughness height (m)
z_{oms}	Equivalent roughness length of the underlying bare soil in absence of vegetation (m)
z_v	Vegetation height (m)
α_0	Coefficient in r_{av}
α_s	Soil albedo
α_v	Vegetation albedo
β	Evapotranspiration efficiency
β_s	Evaporation efficiency
$\beta_{s,e}$	Merlin et al. (2011) evaporation efficiency
β_v	Transpiration efficiency
ϵ_s	Emissivity of the soil
ϵ_v	Emissivity of the vegetation
Δ	Slope of the vapour pressure deficit at T_a
γ	Psychrometric constant ($Pa K^{-1}$)
ρ	Air density ($kg m^{-3}$)
σ	Stefan–Boltzmann constant ($W m^{-2} K^{-4}$)
θ_{0-5cm}	Integrated volumetric soil moisture in the top 5 cm
θ_{sat}	Volumetric soil moisture at saturation

Title Page

Abstract

Introduction

Conclusions

References

Tables

Figures

⏪

⏩

◀

▶

Back

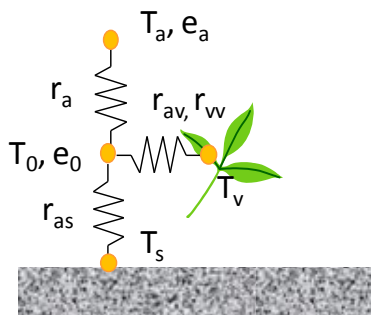
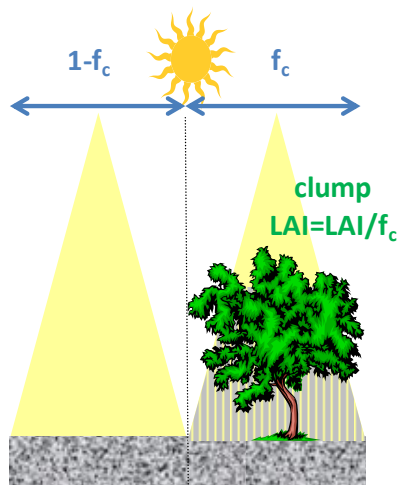
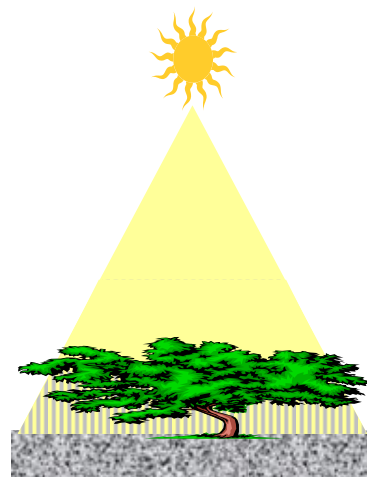
Close

Full Screen / Esc

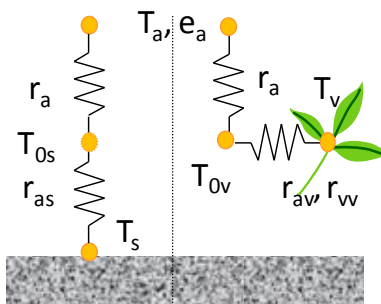
Printer-friendly Version

Interactive Discussion





Series



Parallel

Figure 1. Schematic showing the series and parallel model approaches.

Title Page

Abstract

Introduction

Conclusions

References

Tables

Figures

◀

▶

◀

▶

Back

Close

Full Screen / Esc

Printer-friendly Version

Interactive Discussion



SPARSE model for the prediction of evapotranspiration from TIR data

G. Boulet et al.

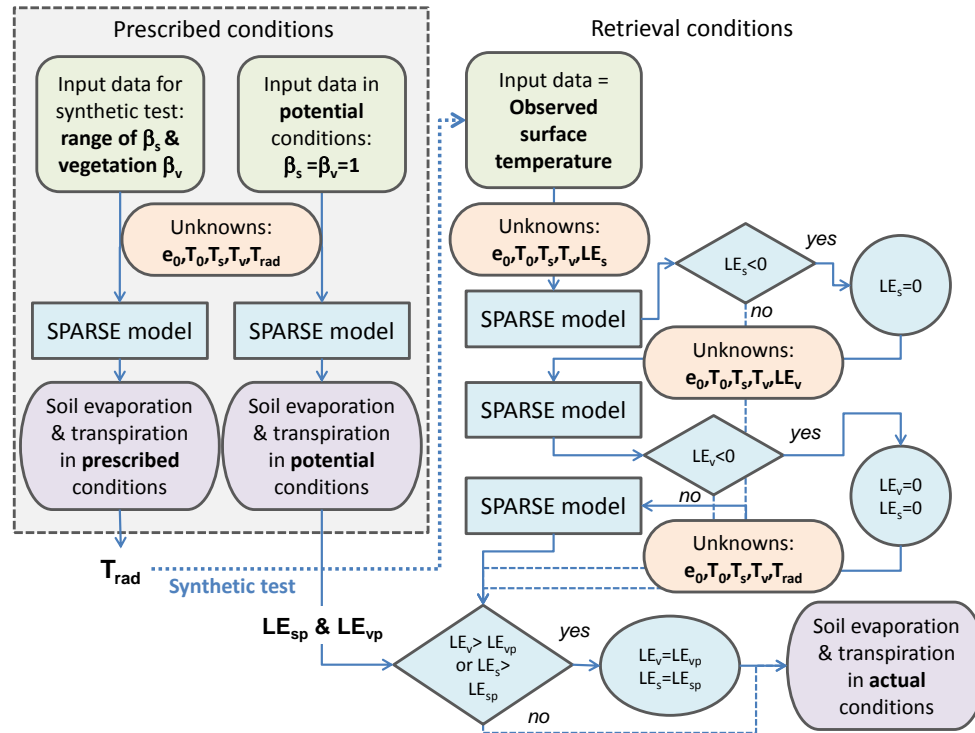


Figure 2. Flowchart of the SPARSE algorithm in prescribed and retrieval conditions.

Title Page

Abstract Introduction

Conclusions References

Tables Figures

◀ ▶

◀ ▶

Back Close

Full Screen / Esc

Printer-friendly Version

Interactive Discussion



SPARSE model for the prediction of evapotranspiration from TIR data

G. Boulet et al.

Title Page

Abstract

Introduction

Conclusions

References

Tables

Figures

◀

▶

◀

▶

Back

Close

Full Screen / Esc

Printer-friendly Version

Interactive Discussion

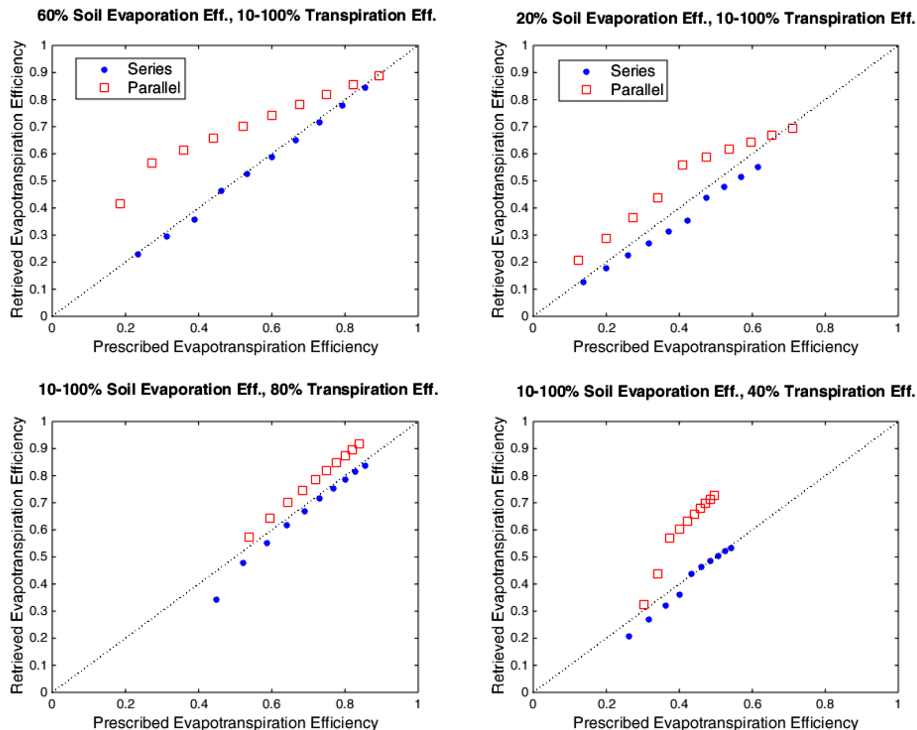


Figure 3. Retrieval test for total evapotranspiration (β) efficiency when using T_{rad} values as input to SPARSE for given combinations of prescribed β_s and β_v values.

SPARSE model for the prediction of evapotranspiration from TIR data

G. Boulet et al.

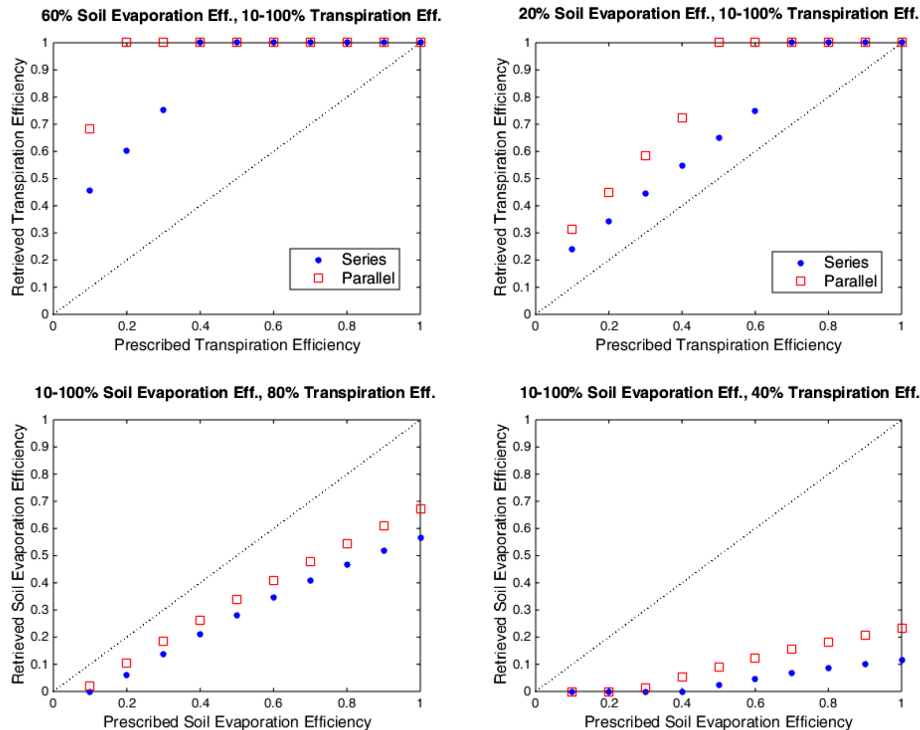


Figure 4. Retrieval test for component evapotranspiration (β_s , β_v) efficiencies when using T_{rad} values as input to SPARSE for given combinations of prescribed β_s and β_v values.

[Title Page](#)
[Abstract](#) [Introduction](#)
[Conclusions](#) [References](#)
[Tables](#) [Figures](#)
⏪ ⏩
◀ ▶
[Back](#) [Close](#)
[Full Screen / Esc](#)
[Printer-friendly Version](#)
[Interactive Discussion](#)



**SPARSE model for
the prediction of
evapotranspiration
from TIR data**

G. Boulet et al.

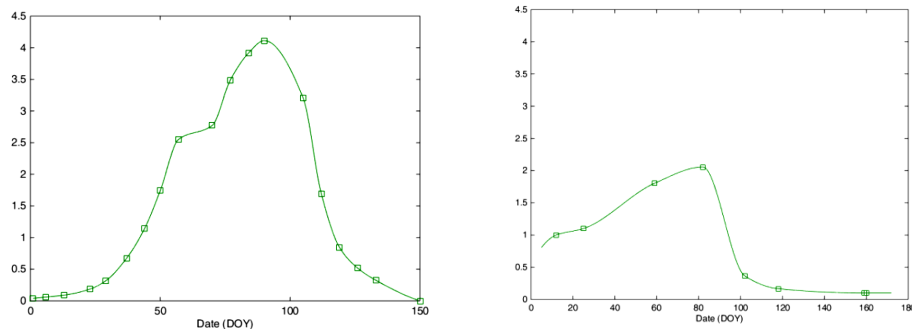


Figure 5. Evolution of leaf area index in the irrigated wheat (left) and rainfed wheat (right) sites.

[Title Page](#)[Abstract](#)[Introduction](#)[Conclusions](#)[References](#)[Tables](#)[Figures](#)[◀](#)[▶](#)[◀](#)[▶](#)[Back](#)[Close](#)[Full Screen / Esc](#)[Printer-friendly Version](#)[Interactive Discussion](#)

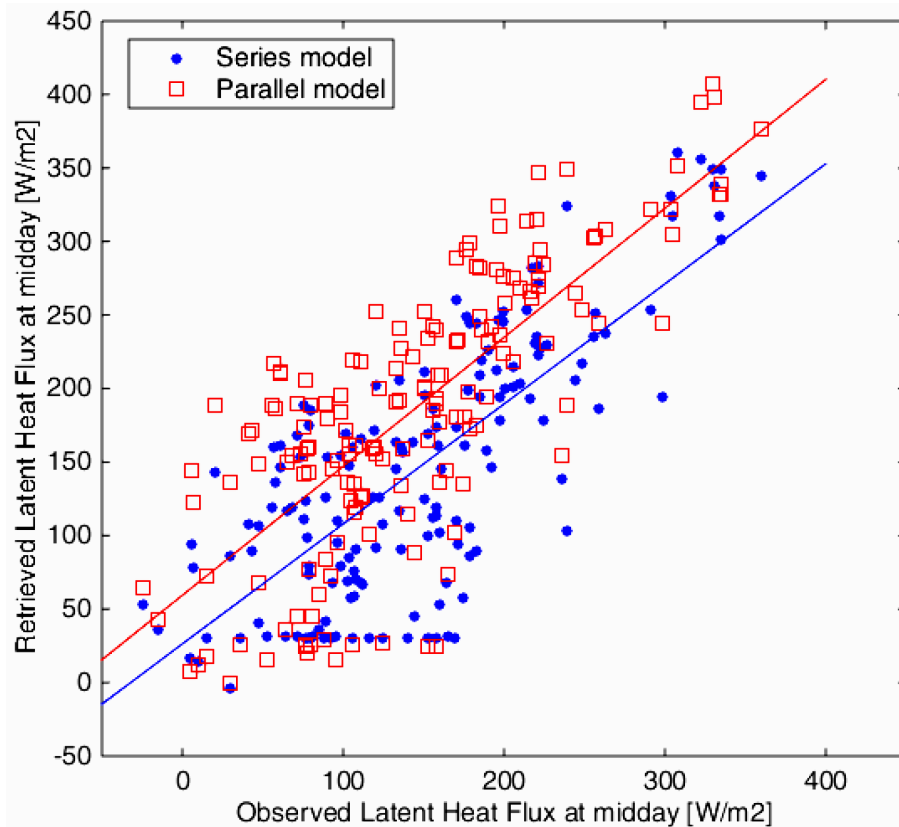


Figure 6. Scatterplot of retrieved vs. observed latent heat flux at midday at the rainfed wheat site.

HESSD

12, 7127–7178, 2015

SPARSE model for the prediction of evapotranspiration from TIR data

G. Boulet et al.

Title Page

Abstract

Introduction

Conclusions

References

Tables

Figures

◀

▶

◀

▶

Back

Close

Full Screen / Esc

Printer-friendly Version

Interactive Discussion



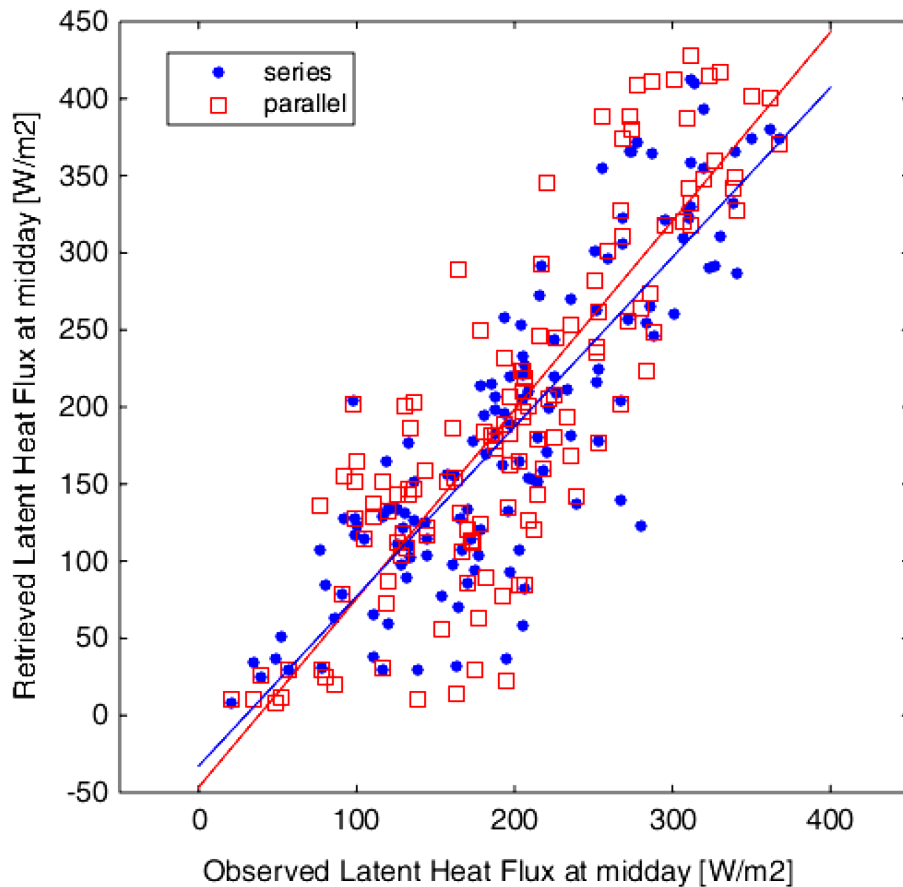


Figure 7. Same as Fig. 6 for the irrigated wheat site.

HESSD

12, 7127–7178, 2015

SPARSE model for the prediction of evapotranspiration from TIR data

G. Boulet et al.

Title Page	
Abstract	Introduction
Conclusions	References
Tables	Figures
⏪	⏩
◀	▶
Back	Close
Full Screen / Esc	
Printer-friendly Version	
Interactive Discussion	



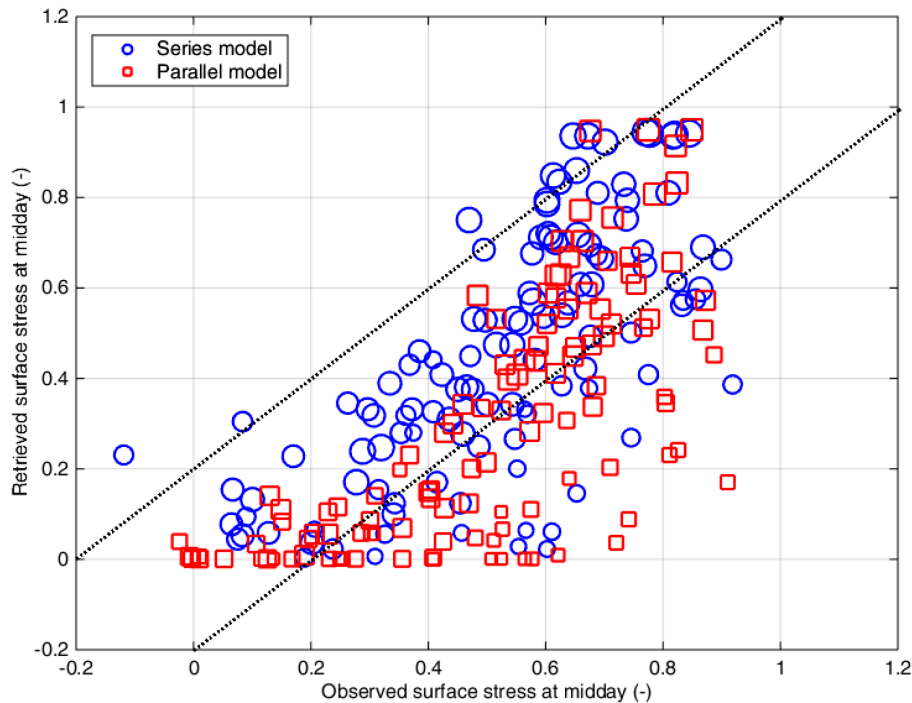


Figure 8. Scatterplot of retrieved vs. observed surface bounded water stress at midday at the rainfed wheat site (marker size proportional to potential evapotranspiration).

SPARSE model for the prediction of evapotranspiration from TIR data

G. Boulet et al.

[Title Page](#)

[Abstract](#)

[Introduction](#)

[Conclusions](#)

[References](#)

[Tables](#)

[Figures](#)

[⏪](#)

[⏩](#)

[◀](#)

[▶](#)

[Back](#)

[Close](#)

[Full Screen / Esc](#)

[Printer-friendly Version](#)

[Interactive Discussion](#)



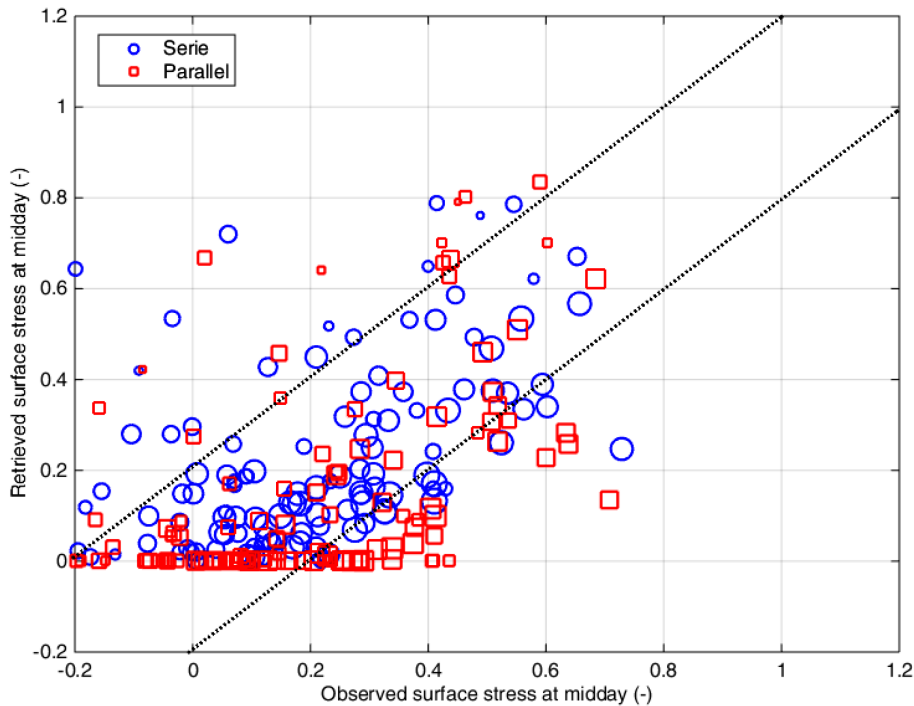


Figure 9. Same as Fig. 8 for the irrigated wheat site.

SPARSE model for the prediction of evapotranspiration from TIR data

G. Boulet et al.

Title Page

Abstract

Introduction

Conclusions

References

Tables

Figures

◀

▶

◀

▶

Back

Close

Full Screen / Esc

Printer-friendly Version

Interactive Discussion



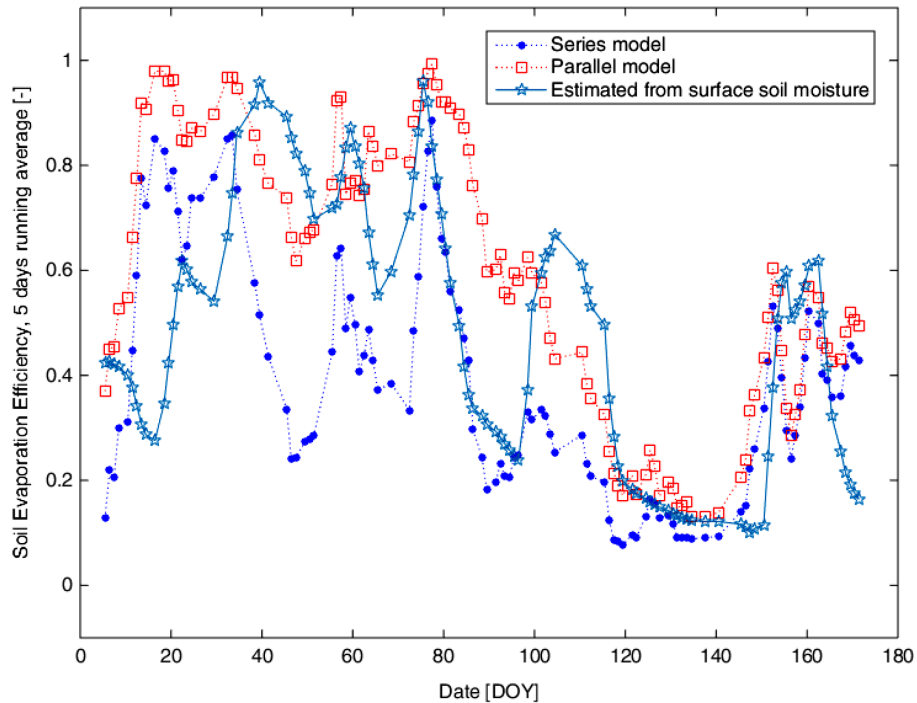


Figure 10. Evolution of the retrieved evaporation efficiencies compared to the simulated evaporation efficiency computed using observed surface soil moisture time series for the rainfed wheat site.

SPARSE model for the prediction of evapotranspiration from TIR data

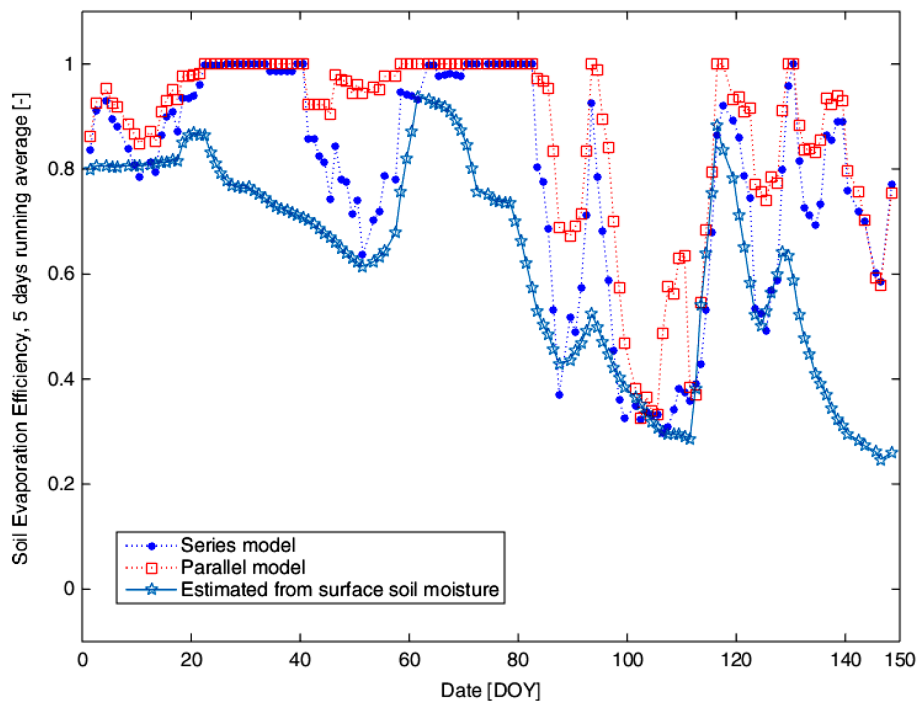
G. Boulet et al.

Title Page	
Abstract	Introduction
Conclusions	References
Tables	Figures
◀	▶
◀	▶
Back	Close
Full Screen / Esc	
Printer-friendly Version	
Interactive Discussion	



**SPARSE model for
the prediction of
evapotranspiration
from TIR data**

G. Boulet et al.

**Figure 11.** Same as Fig. 10 for the irrigated wheat site.[Title Page](#)[Abstract](#)[Introduction](#)[Conclusions](#)[References](#)[Tables](#)[Figures](#)[◀](#)[▶](#)[◀](#)[▶](#)[Back](#)[Close](#)[Full Screen / Esc](#)[Printer-friendly Version](#)[Interactive Discussion](#)